Astron. Astrophys. 321, 444–451 (1997)

ASTRONOMY
AND
ASTROPHYSICS

An analytical method for inferring the law of gravity from the macroscopic dynamics: Spherical and thin-disk mass distributions with exponential density

C. Rodrigo-Blanco

Laboratorio de Astrofísica Espacial y Física Fundamental (LAEFF), P.O. Box 50727, E-28080 Madrid, Spain (crb@laeff.esa.es)

Received 29 July 1996 / Accepted 17 October 1996

Abstract. We consider the gravitational potential and the gravitational rotation field generated by a mass distribution with exponential density, when the force between any two mass elements is not the usual Newtonian one, but some general central force. The usual integral relations are inverted and the elemental interaction (between two point-like masses) is obtained as a function of the macroscopic gravitational field (the one generated by the distribution). This has been done in two cases of interest: a sphere, where the exact solution has been found, and a thin disk, where the problem has been solved in the *Gaussian* approximation. This approach gives us a direct way for testing the possibility of finding a correction to the Newtonian law of gravity that can explain the observed dynamics at large scales without the need of dark matter. We also show that the solution for the thin disk, in the *Gaussian* approximation, can be used in the case of spiral galaxies with a good level of confidence.

Key words: gravitation – galaxies: kinematics and dynamics – methods: analytical – cosmology: dark matter

1. Introduction

The dynamical analysis of rotation curves of galaxies, binary galaxies, clusters of galaxies and large scales structures show significant discrepancies between the observed behaviour and the one expected from the application of General Relativity and its Newtonian limit to the visible mass. This disagreement has led many astrophysicists to believe in the existence of a large amount of non-visible matter and is, thus, commonly known as the *"dark matter problem"*.

In spite of this, there is no direct evidence for the validity of either Einstein's General Relativity or Newtonian gravity at scales much larger than those of the Solar system (See, e.g., Will 1993). There is, therefore, no experimental or observational reason to ascertain that unmodified General Relativity holds at larger distances. This leads us to think that we should be open to the possibility that it had to be revised (perhaps in the same spirit as Newton's law had to be modified for strong fields and large velocities).

In this paper we consider the possibility that Newton's law of gravity is just a good approximation at short distances of a more general expression for the force. It is interesting to identify which, if any, extensions of the usual inverse square law are compatible with the dynamics observed at large scales.

Work along these lines has already been done (Tolhine 1983, Kuhn & Kruglyak 1987, Mannheim & Kazanas 1989) assuming a specific functional form for the force, and then evaluating the field generated by a mass distribution (for instance, a galaxy) by performing the corresponding three-dimensional integrals. This approach has helped to find very interesting results, as the scale (5 - 10 kpc) where the breakdown of Newtonian gravity takes place when the correction to the force is assumed to be proportional to $1/r$ (Kuhn & Kruglyak 1987), but its success obviously depends on the election of the initial form for the force. We present and work out a method that allows us to follow the inverse methodology, that is, to infer, directly from observations, the phenomenological law of gravity that is able to generate a given macroscopic gravitational field. We do it for the cases of a spherical mass distribution and a thin disk with exponential density.

In Sect. 2 we give the general definitions that will be used later in Sect. 3 for the case of spherical symmetry, and in Sect. 4 for a thin disk (in both cases assuming an exponential density). In Sect. 5 we study the possibility of using the results obtained in the previous sections to study the problem of rotation curves of spiral galaxies under a non-Newtonian point of view, and in Sect. 6 an example is shown on how to use these results for a real galaxy. Finally, some conclusions are offered. In Appendix A we show the mathematical basis underlying the results presented in Sects. 3 and 4.

2. General definitions

Let us assume that the gravitational potential generated by a point-like mass does not correspond to the usual Newtonian form but can be written in terms of a function $g(r)$ that describes the deviation from the Newtonian law, that is,

$$\phi(r) \equiv -\frac{G_0 m_1 m_2}{r} g(r). \tag{1}$$

where $\phi(r)$ is the gravitational potential experienced by two point-like particles of masses m_1 and m_2 separated by a distance r and G_0 is the Newton's constant. Of course, the Newtonian limit, $g(r) \to 1$, must be recovered as $r \to 0$.

This modification could, for example, be due to the many body nature of the mass distribution making up the galaxy, a relativistic theory different from General Relativity... This is irrelevant in what follows.

The force per unit mass is, by definition, the gradient of the potential,

$$\boldsymbol{F}(r) \equiv -\frac{G_0 m_1 m_2}{r^2} g_{\text{eff}}(r)\frac{\boldsymbol{r}}{r}, \tag{2}$$

where we have introduced

$$g_{\text{eff}}(r) \equiv g(r) - r g'(r). \tag{3}$$

with $g_{\text{eff}}(r) \to 1$ as $r \to 0$, as required by the Newtonian limit.

In this way, to find the total potential or the total force generated by a mass distribution Ω with density $\rho(\boldsymbol{r})$, one must integrate over the volume spanned by Ω to get:

$$\Phi(\boldsymbol{R}) = -G_0 \int\int\int_{\Omega} d^3\boldsymbol{r}\ \frac{g(|\boldsymbol{R}-\boldsymbol{r}|)}{|\boldsymbol{R}-\boldsymbol{r}|}\ \rho(\boldsymbol{r}) \tag{4}$$

for the potential experienced by a point mass at a distance R from the centre of Ω, and

$$\boldsymbol{F}(\boldsymbol{R}) = -G_0 \int\int\int_{\Omega} d^3\boldsymbol{r}\ \frac{g_{\text{eff}}(|\boldsymbol{R}-\boldsymbol{r}|)}{|\boldsymbol{R}-\boldsymbol{r}|^2}\ \frac{\boldsymbol{R}-\boldsymbol{r}}{|\boldsymbol{R}-\boldsymbol{r}|}\ \rho(\boldsymbol{r}) \tag{5}$$

for the force.

In the case that the gravitational potential is only a function of the distance to the centre of the distribution, it is convenient to introduce two new functions $\Psi(R)$ and $\Psi_{\text{eff}}(R)$ such that:

$$\Phi(R) \ \equiv\ -\frac{G_0 M_{\text{tot}}}{R}\ \Psi(R), \tag{6}$$

$$\boldsymbol{F}(R) \ \equiv\ -\frac{G_0 M_{\text{tot}}}{R^2}\ \Psi_{\text{eff}}(R)\ \frac{\boldsymbol{R}}{R}, \tag{7}$$

and the rotation velocity of a test particle in a circular orbit bound to the distribution will be:

$$V^2_{\text{rot}}(R) \ \equiv\ \frac{G_0 M_{\text{tot}}}{R}\ \Psi_{\text{eff}}(R) \tag{8}$$

where the auxiliary functions $\Psi_{\text{eff}}(R)$ and $\Psi(R)$ satisfy the following functional relationship:

$$\Psi_{\text{eff}}(R) = \Psi(R) - R\Psi'(R), \tag{9}$$

Our goal is to design a procedure where, assuming that $\boldsymbol{F}(R)$ is known (say from observation of the rotation velocity) for all values of R, we obtain a $g_{\text{eff}}(r)$ that generates the given rotation velocity. Or, in other words, given the potential as inferred from observations we want to find which $g(r)$ could have generated it. Actually, what we will find are $g(r)$ and $g_{\text{eff}}(r)$ as functions of $\Psi(R)$ and $\Psi_{\text{eff}}(R)$ respectively. This will be done, in the following sections, for the cases of spherical symmetry and a thin disk, in both cases assuming an exponential density.

3. Spherical mass distribution with exponential density

In this section, we study a spherically symmetric distribution with an exponentially decaying density:

$$\rho(r) \equiv \rho_0\ e^{-\alpha r}. \tag{10}$$

Our ultimate goal is to find a method to study the discrepancies between the observed rotation curves of spiral galaxies and the curves predicted by using Newton's law of gravity. The luminosity profile of many spiral galaxies can be well fitted assuming that the density of luminous matter decreases exponentially with distance from the centre of the galaxy (Kent 1987). This is the reason why we are interested in studying such a density function, even though spiral galaxies are not, obviously, spherical.

Using Eqs. (6), (7) and (10), in Eqs. (4) and (5), and considering spherical symmetry, the two problems sketched in Sect. 2 can be conveniently recast in the form of two integral equations:

(i) Given $\Psi(R)$, find a function $g(r)$ that satisfies the equation:

$$\int_0^\infty dr \int_0^\pi d\theta \int_0^{2\pi} d\phi \frac{g(\sqrt{R^2+r^2-2Rr\cos\theta})}{\sqrt{R^2+r^2-2Rr\cos\theta}} r^2 \sin\theta e^{-\alpha r} = \frac{8\pi}{\alpha^3}\frac{\Psi(R)}{R} \tag{11}$$

and

(ii) Given $\Psi_{\text{eff}}(R)$, find a function $g_{\text{eff}}(r)$ such that:

$$\int_0^\infty dr \int_0^\pi d\theta \int_0^{2\pi} d\phi \frac{g_{\text{eff}}(\sqrt{R^2+r^2-2Rr\cos\theta})}{(R^2+r^2-2Rr\cos\theta)^{\frac{3}{2}}} \times\ (R - r\cos\theta) r^2 \sin\theta e^{-\alpha r} \ =\ \frac{8\pi}{\alpha^3}\frac{\Psi_{\text{eff}}(R)}{R^2}. \tag{12}$$

The solution to these integral equations will be described in detail in Appendix A.1 The results can be summarised as:

(i) Potential problem (*viz.* Eqs. (6) and (11))

In this case, the exact solution to the problem is

$$g(x) = \Psi(x) - \frac{2}{\alpha^2}\Psi''(x) + \frac{1}{\alpha^4}\Psi^{(iv)}(x) \tag{13}$$

where the function Ψ has the following behaviour at the origin:

$$\Psi(0) \ =\ \Psi''(0) \ =\ 0. \tag{14}$$

(ii) Force and velocity problem (*viz.* Eqs. (7), (8) and (12)).

Here, the exact solution is given by the following expression:

$$g_{\rm eff}(x) = \Psi_{\rm eff}(x) - \tfrac{2}{\alpha^2}\Psi''_{\rm eff}(x) + \tfrac{1}{\alpha^4}\Psi^{(iv)}_{\rm eff}(x) + \tfrac{4}{\alpha^2 x}\Psi'_{\rm eff}(x) - \\ - \tfrac{4}{\alpha^4 x^4}\left[2x\Psi'_{\rm eff}(x) - 2x^2\Psi''_{\rm eff}(x) + x^3\Psi'''_{\rm eff}(x)\right] \quad (15)$$

The behaviour of Ψ at the origin is as follows:

$$\Psi_{\rm eff}(0) = \Psi'_{\rm eff}(0) = \Psi''_{\rm eff}(0) = 0. \quad (16)$$

The behaviours at the origin just tell us that $\Psi_{\rm eff}(R) \propto R^3$ for $R \sim 0$, and thus, $V_{\rm rot}(R) \propto R$ for $R \sim 0$, which is in fact in good agreement with the observations (as the observed rotation curves are usually well fitted in the inner regions by a straight line) and, from a non-Newtonian gravity point of view, it is also in agreement with the fundamental experimental constrain that for short distances the gravitational interaction must be well described by a Newtonian limit.

4. Thin-disk mass distribution with exponential density

The luminosity profile of many spiral galaxies can be well fitted assuming that the luminous matter is placed along a thin disk with a density that decreases exponentially with the distance to the centre of the galaxy (Kent 1987).

$$\rho(r,z) \equiv \sigma_0\, \delta(z)\, e^{-\alpha r}. \quad (17)$$

being σ_0 a normalisation constant with units of a two-dimensional density, related to the total mass of the galaxy by $M_{\rm tot} = 2\pi\sigma_0\alpha^{-2}$.

Considering a thin-disk distribution and using Eqs. (6), (7) and (17), in Eqs. (4) and (5), the two problems outlined in Sect. 2 can be recast as two integral equations:

(i) Given $\Psi(R)$, defined by (6), find a function $g(r)$ such that:

$$\int_0^\infty dr \int_0^{2\pi} d\theta \frac{g(\sqrt{R^2+r^2-2Rr\cos\theta})}{\sqrt{R^2+r^2-2Rr\cos\theta}}\, r\, e^{-\alpha r} = \\ = \frac{2\pi}{\alpha^2}\frac{\Psi(R)}{R}. \quad (18)$$

(ii) Given $\Psi_{\rm eff}(R)$, defined by (7), find a function $g_{\rm eff}(r)$ such that:

$$\int_0^\infty dr \int_0^{2\pi} d\theta \frac{g_{\rm eff}(\sqrt{R^2+r^2-2Rr\cos\theta})}{(R^2+r^2-2Rr\cos\theta)^{\frac{3}{2}}}(R - r\cos\theta) r\, e^{-\alpha r} = \\ = \frac{2\pi}{\alpha^2}\frac{\Psi_{\rm eff}(R)}{R^2}. \quad (19)$$

In this case the problem cannot be solved exactly. We use an approximation that we call *Gaussian* as, in the Newtonian case, it is equivalent to use the Gauss' law for calculating the gravitational field.

The calculations are described in detail in Appendix A.2. The solution to the two problems outlined above, in the *Gaussian approximation* can be summarised as:

(i) Potential problem: (*viz.* Eqs. (6) and (18))

In this case, the approximate solution to the problem is

$$g(x) = \Psi(x) - \frac{1}{\alpha^2}\Psi''(x), \quad (20)$$

where the function Ψ has the following behaviour at the origin:

$$\Psi(0) = 0. \quad (21)$$

(ii) Force and velocity problem: (*viz.* Eqs. (7), (8) and (19)).

Here, the approximate solution is given by the following expression:

$$g_{\rm eff}(x) = \Psi_{\rm eff}(x) - \frac{1}{\alpha^2}\Psi''_{\rm eff}(x) + \frac{2}{\alpha^2 x}\Psi'_{\rm eff}(x) \quad (22)$$

and the behaviour of Ψ at the origin is as follows:

$$\Psi_{\rm eff}(0) = \Psi'_{\rm eff}(0) = 0. \quad (23)$$

5. Real thin disks: comparison between the spherical and the Gaussian approximations

In this section we consider the possibility of using the results obtained in the previous sections to study the rotation curves of spiral galaxies (provided they can be described as thin disks with exponential density).

At first sight, we would think that we cannot apply the results of Sect. 3 to spiral galaxies, because they have been obtained assuming spherical symmetry, and spiral galaxies are disk-shaped, not spherical. In spite of this, it seems logical that the difference between the gravitational field generated by a sphere and the one generated by a disk becomes negligible at very large distances (here "large distances" means large compared with some typical length scale for the distribution; it could be, for instance, α^{-1}, i.e, the exponential length scale of the mass distribution). Furthermore, when we consider the effect of an increasing $g_{\rm eff}(r)$, it is evident that the meaning of what is a "large distance" changes as we change the functional form of $g_{\rm eff}(r)$. That is, the faster $g_{\rm eff}(r)$ grows as a function of r, the smaller the distance at which a sphere is indistinguishable from a disk becomes, when considered from the gravitational point of view.

Concerning the solution summarised in Sect. 4 for a thin disk, it is not an exact solution to the problem. In Appendix A.2 the details are shown, but the main point is that in the step from Eq. (A17) to Eq. (A18) we made the approximation of considering only the first term of an infinite series. The terms dropped depend also on $g(r)$, which is not known, so it is not trivial to evaluate the goodness of the approximation.

In this section, we choose some functions $g_{\rm eff}(r)$ and compare the *exact* rotation velocity with the two *approximate* ones: (i) approximating a disk with a sphere, and (ii) using the *Gaussian* approximation for the thin disk. By *exact* we mean the rotation velocity generated by the considered $g_{\rm eff}(r)$ through Eqs. (19) and (8). Nevertheless, for most functional forms of $g_{\rm eff}(r)$ an analytical solution cannot be found and it is necessary to perform numerical integrations for finding that *exact* rotation velocity. Whenever that happens, we have decided to perform

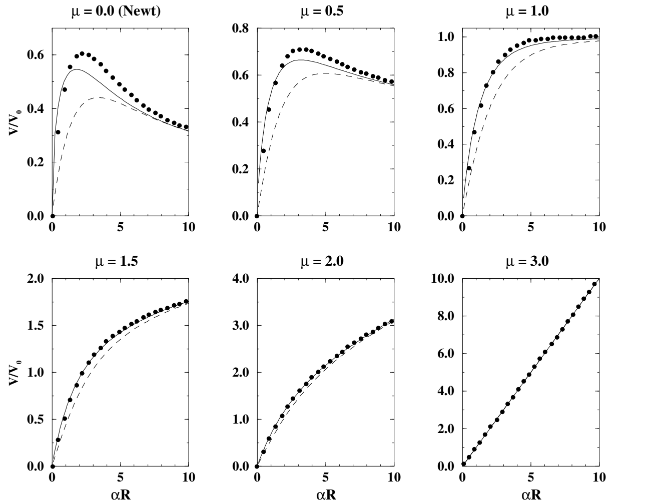

Fig. 1. Exact rotation curves (dots), *Gaussian* approximation (solid line) and *spherical* approximation (dashed line) when $g_{\rm eff}(r) \equiv \left(\frac{r}{a}\right)^{\mu}$ for some values of μ (μ = 0 is the Newtonian case). In every case, for the sake of clarity, the velocities are normalised by dividing by an appropriate constant $V_0 \equiv \left(\frac{G_0 M_{\rm tot}\alpha}{(\alpha a)^{\mu}}\right)^{1/2}$.

the integrals assuming that the disk has some non-zero thickness. Actually, this is a more realistic model for a spiral galaxy, the astrophysical system to which our approximate method is applied.

By *approximate* rotation velocity we mean the one such that the corresponding $\Psi_{\rm eff}(R)$ satisfies the adequate equations: Eqs. (15) and (16) (for the spherical approximation); and Eqs. (22) and (23) for the *Gaussian* one.

Concerning the *Gaussian* approximation, as a test of consistency, we first consider the Newtonian case, i.e., $g(r) = g_{\rm eff}(r) = 1$. When Eqs. (22) and (23) are used we obtain:

$$\Psi_{\rm eff}(R) = 1 - (1+\alpha R)e^{-\alpha R}, \quad (24)$$

and thus, the rotation velocity is

$$V^2_{\rm rot}(R) = \frac{G_0 M_{\rm tot}}{R}[1-(1+\alpha R)e^{-\alpha R}] = \frac{G_0 M(R)}{R}, \quad (25)$$

where $M(R)$ is the disk mass inside the sphere of radius R. Of course, this is not the exact result, but it is what we find if we apply the Gauss' law as an approximation for evaluating the gravitational field. That is why the approximation is called *Gaussian*.

Next, both approximations must be checked for other different forms of $g_{\rm eff}$. For doing that we choose a parametric family of $g_{\rm eff}(r)$'s given by

$$g_{{\rm eff},\mu}(r) \equiv \left(\frac{r}{a}\right)^{\mu}, \quad (26)$$

where μ parametrises how fast $g_{\rm eff}$ grows.
We have found the *exact* analytical solution (for the thin-disk case) for $\mu = 1$ and $\mu = 3$:

$$V^2_{{\rm rot},\mu=1}(R) = \frac{G_0 M_{\rm tot}}{a}[1-(1+\alpha R)e^{-\alpha R}] = \frac{G_0 M(R)}{R}\ \frac{R}{a}, \quad (27)$$

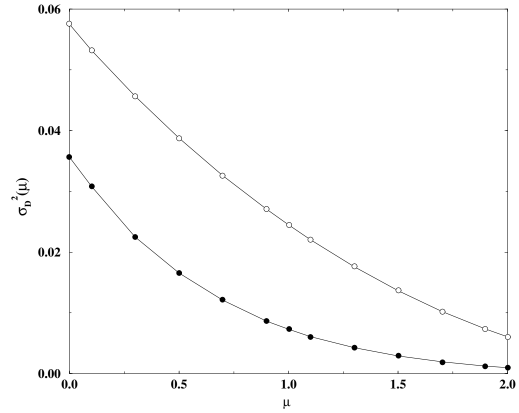

Fig. 2. Mean square error in the velocity when the *Gaussian* (full points) and the spherical approximation (open points) are used instead of the exact solution for the disk, as a function of μ, and using $g_{\rm eff}(r) \equiv \left(\frac{r}{a}\right)^{\mu}$. The exact meaning of $\sigma^2_{\rm D}$ is explained in the text.

$$V^2_{{\rm rot},\mu=3}(R) = \frac{G_0 M_{\rm tot}}{R}\ \left(\frac{R}{a}\right)^3\left(1+\frac{6}{\alpha^2 R^2}\right). \quad (28)$$

For the other values of μ the integrals are performed numerically for a disk with a small thickness $h = \alpha^{-1}/6$

In the Gaussian approximation, it can be seen that, for $\mu = 3$ the solution is (28), that is, the approximation is exact.

In Fig. 1 we have plotted the exact rotation velocities compared with those corresponding to both approximations for some values of μ. For each case, the solutions are normalised dividing by a convenient constant V_0 defined as:

$$V_0 \equiv \left(\frac{G_0 M_{\rm tot}\alpha}{(\alpha a)^{\mu}}\right)^{\frac{1}{2}}. \quad (29)$$

It can be seen in Fig. 1 that the *Gaussian* approximation (that is always better than the *spherical* one) is quite good in every case, and is better when $g_{\rm eff}(r)$ is a growing function of r. However, it would be interesting to have a more quantitative way of describing the difference in the rotation velocity obtained in the exact case and in both approximations as a function of μ. In order to do that, we define the quantity σ^2 as follows:

$$\sigma^2(\mu) \equiv \frac{1}{N}\sum_{i=1}^{N}\frac{(V_{{\rm D},\mu}(r_i) - V_{{\rm A},\mu}(r_i))^2}{V^2_{{\rm D},\mu}(r_i)}, \quad (30)$$

where the sub-scripts D and A stand for the disk (exact) and the approximation (either the spherical or the *Gaussian* one) respectively. We sum over r_i, which are the points where the integrals are calculated. The total number of points for each value of μ is $N = 100$.

So defined, $\sigma^2(\mu)$ is a measure of the mean square error that we make in the rotation velocity if the approximation is used instead of the numerical integrals, for each value of μ.

In Fig. 2, we plot the value of σ^2 versus μ. As a result of what is seen in Figs. 1 and 2 two conclusions can be extracted: (i) the *Gaussian* approximation is a much better tool for studying

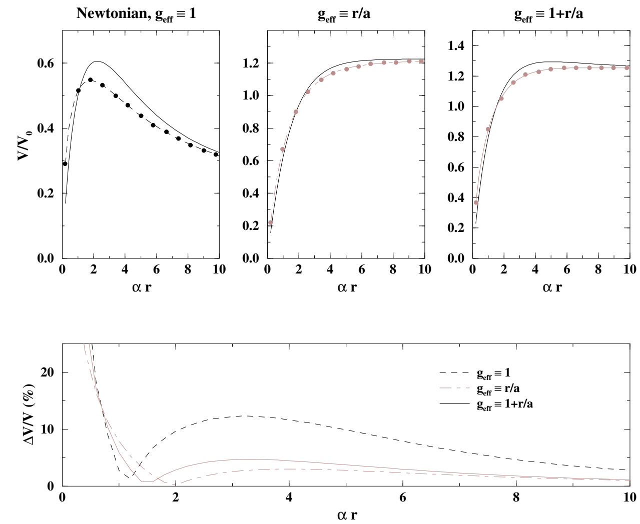

Fig. 3. Comparison between the exact rotation curve and the one in Gaussian approximation, for a galaxy with length scale $r_{\rm d} = 3kpc$, for three cases of interest: $g_{\rm eff} = 1$, $g_{\rm eff} = r/a$, $g_{\rm eff} = 1 + r/a$, being $a \equiv 2kpc$. All the curves are normalised dividing by $V_0 \equiv (G_0 M_{\rm tot}/r_{\rm d})^{1/2}$ The lower graph shows the percentage of difference between both curves in the three cases.

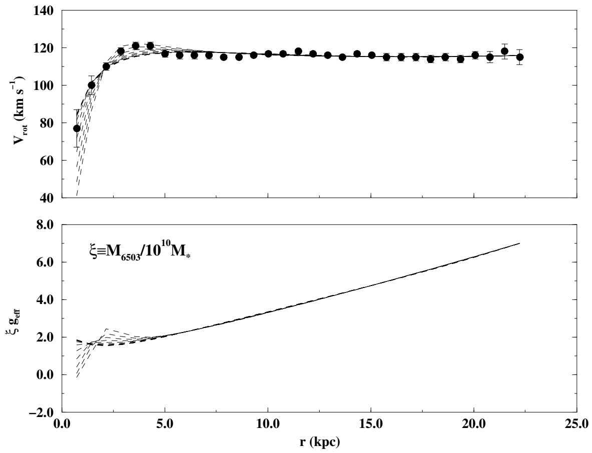

Fig. 4. Fits of the rotation curve of NGC 6503 using twelve different functional forms (We have used the class of functions v_λ, defined in Eq. (31), with a third-degree polynomial and twelve different values of λ going from 1.0 to 2.2 (upper graph) and the $g_{\rm eff}(r)$ corresponding to each fit (lower graph).

the gravitational field in thin disk galaxies, and (ii) the faster $g_{eff}(r)$ grows with r, the better is the approximation.

There remains the problem that $g_{\rm eff}$ must be Newtonian for small distances and thus, the fact that the *Gaussian* approximation is not very good for the Newtonian case could introduce large errors in the final results. We have calculated the exact curve and the one corresponding to the *Gaussian* approximation in the simple, but interesting, case when $g_{\rm eff} \equiv 1+r/a$, for a galaxy with a length scale $r_{\rm d} = \alpha^{-1}$ = 3kpc and we have taken $a \equiv 2$ kpc which is consistent with the $g_{\rm eff}$ that is obtained in Rodrigo-Blanco & Pérez-Mercader (1997) when working with real data. In Fig. 3 we have plotted the rotation curve for this $g_{\rm eff}$ compared with the Newtonian one and the one for $g_{\rm eff} = r/a$. We also have plotted the value of $|\Delta V/V|$ defined as:

$$\left|\frac{\Delta V}{V}\right| \equiv \left|\frac{V_{\rm D} - V_{\rm A}}{V_{\rm D}}\right| \tag{31}$$

where $V_{\rm D}$ stands for the exact disk solution and $V_{\rm A}$ is the velocity in the *Gaussian* approximation. It can be seen that, although the error in the Newtonian case can reach a 15%, the final error for $g_{\rm eff} = 1+r/a$ is more than three times smaller. This is due to the fact that for distances of the order of 5 to 10 kpc, $g_{\rm eff}$ begins to be dominated by the non-Newtonian contribution and thus the approximation becomes more accurate.

6. An example of how to work with real data

In this section we just give a simple example of how to use the results previously obtained to study the problem of the rotation curves of spiral galaxies under a non-Newtonian point of view. We will do it only for one galaxy, just to show how the method can be used. In a forthcoming paper (Rodrigo-Blanco & Pérez-Mercader 1997) a similar and more detailed study of a sample of nine galaxies will be done.

We can only apply Eq. (22) to a real galaxy if it can be well described, at least as a first approximation, as a thin disk with exponential density. We have chosen NGC 6503, a galaxy with a luminosity profile that can be well fitted using a thin disk model with exponential density (with a scale length α^{-1} = 1.72 kpc), with no bulge, and without a very large amount of neutral gas (Begeman 1987). Assuming a constant value of M/L for the disk, the luminous mass density of this galaxy can be reasonably described by Eq. (17).

Once we have a galaxy that can be described in the manner described above, the next step is to fit its observed rotation velocity by some mathematical function, so that we can take its derivatives in Eq. (22). It is important to note that there is no physical reason for choosing one function or another to fit the observed data. Thus, we have arbitrarily chosen a functional form for the observed velocity given by:

$$v_\lambda^2(r) = \frac{r^\lambda}{P_3(r)}, \tag{32}$$

where $P_3(r)$ is a third degree polynomial and λ some real number. For twelve values of λ, going from 1.0 to 2.2, the coefficients of the polynomial have been fitted to the observed rotation curve (all the fittings are shown in Fig. 4, upper graph). Once the rotation curve is fitted by a function, Eq. (7) can be used to obtain $M_{\rm tot}\Psi_{\rm eff}$, where $M_{\rm tot}$ is the total mass of the galaxy. In this way, after putting it in Eq. (22), we obtain a form for $M_{\rm tot} g_{\rm eff}$ for each functional fitting. In Fig. 4, lower graph, we have plotted the $g_{\rm eff}$'s corresponding to the fits shown in the upper graph, multiplied by a common factor: $M_{\rm tot}/10^{10} M_\odot$. This $g_{\rm eff}$'s can be introduced into Eq. (2) to obtain an elemental law of gravity (between any two point-like masses) that would generate the observed rotation curve of NGC 6503 without the need of dark matter. The total mass of the galaxy, *a priori*, can be found requiring that $g_{\rm eff}(r=0)=1$. But, actually, Fig. 4 also tells us that the exact form of the elemental force is not constrained by the observed rotation curve at small distances. Thus, since we cannot constrain the exact form of $g_{\rm eff}$ for intermediate distances, we cannot either fix the exact value of the mass of this galaxy.

It must be kept in mind that we are looking for a universal gravitational law, that is, one that is valid for any two point-like particles, with no dependence on where they are located. Thus, the law obtained for one galaxy must be also at work in any other mass distribution. If the laws necessary to explain the rotation curve of other spiral galaxies without dark matter were shown not to be compatible with the one obtained here, that would be a proof against the existence of a law like the one written in Eq. (2).

7. Summary and conclusions

We have found the solution to the problem of inverting the integral relation between the elemental law of gravity and the overall gravitational field generated by two interesting mass distributions: (i) a sphere with exponential density (where the solution is exact), and (ii) a thin-disk with exponential density. The problem in the case of the thin disk has been solved in an approximation that has been called *Gaussian* as it is equivalent to use the Gauss' law for calculating the gravitational field generated by the distribution (that is, to assume that the gravitational force at a distance R to the centre of the disk is proportional to the mass inside that radius). Although this is not exact, we have shown that it is a very good approximation, and it gets much better when $g_{\rm eff}(r)$ grows with r, which is the expected behaviour if the observations must be explained without the need of dark matter. Actually we have also shown that this *Gaussian* approximation is always better than using the results for the case of the sphere as an approximation to the disk case.

In summary, we now have a method for inferring $g_{\rm eff}(r)$ given the observed rotation velocity. It can be said, in some sense, that we have a *way to travel from the world of macroscopic interactions to the world of elemental interactions* (where, by *elemental interaction* we mean that between two point-like particles). It can be sketched as follows: Given the observed $V_{\rm rot}(R)$ for a given galaxy, use Eq. (8) to obtain $\Psi_{\rm eff}(R)$, fit it by a mathematical function and then use Eq. (22) to get the $g_{\rm eff}(r)$ that describes the elemental gravitational force (through Eq. (2)) that can explain the observed rotation curve.

We are now ready for applying the differential expression that we have found to the observed rotation curves of spiral galaxies, and find the $g_{\rm eff}$ required for explaining those rotation curves. We have given an example of how it can be done for a particular galaxy. By repeating the exercise for a sample of several galaxies, we will see whether it is possible or not to find a universal law of gravity that can explain all the rotation curves requiring only the observed luminous matter. This will be done in a separate publication (Rodrigo-Blanco & Pérez-Mercader 1997).

Acknowledgements. I am grateful to Juan Pérez-Mercader for his guidance and help, and also to Massimo Persic and Paolo Salucci for their hospitality at SISSA, where a part of this work has been done, and for their helpful comments. I would also like to thank the referee for his help in improving this paper.

Appendix A: mathematical development

The line for the proof of Eqs. (13, (14), (15), and (16), for the spherical mass distribution, is very similar to the one for the proof of Eqs. (20, (21), (22), and (23), for the thin disk. Thus, the calculations are first shown in some detail for the sphere (where the solution is exact) and, then, the main differences for the case of the disk are explained.

A.1. Sphere with exponential density

First, we show the solution to what we call *the potential problem*, that is, how to go from Eq. (11) to Eqs. (13) and (14). Later we will use these results to solve *the force problem*, i.e, how to go from Eq. (12) to Eqs. (15) and (16).

In order to go from equation Eq. (11) to Eqs. (13) and (14), it is convenient to work with the integration variables in a way that is as independent as possible of the form of the function g. In order to do this, it is useful to use the Fourier sine transform:

$$g(\omega) \equiv \frac{2}{\pi}\int_0^\infty \hat{g}_s(p)\sin(p\omega)dp, \tag{A1}$$

as this allow us to use the addition theorem for Bessel functions (see Gradshteyn 1980) for decoupling the integration variables in the integrals:

$$\frac{\sin(p\omega)}{\omega} = \frac{\pi}{2\sqrt{Rr}}\sum_{\rm k=0}^{\infty}(2k+1)J_{\rm k+\frac{1}{2}}(pr)J_{\rm k+\frac{1}{2}}(pR)P_k(\cos\theta)$$
$$\text{where:}\quad \begin{cases}\omega \equiv \sqrt{r^2+R^2-2rR\cos\theta}\\ P_k \equiv \text{Legendre Polynomials.}\end{cases} \tag{A2}$$

Making use of all these equations, Eq. (11) can now be written as:

$$\frac{\Psi(R)}{R} = \frac{\alpha^3}{4}\int_0^\infty dr\int_0^\infty dp\,\hat{g}_s(p)\,r^2e^{-\alpha r}\sum_{\rm k=0}^{\infty}(2k+1)$$
$$\times\ \frac{J_{\rm k+\frac{1}{2}}(pR)}{\sqrt{R}}\frac{J_{\rm k+\frac{1}{2}}(pr)}{\sqrt{r}}\int_0^\pi d\theta P_k(\cos\theta)\sin\theta. \tag{A3}$$

And, then, the orthogonality of Legendre polynomials,

$$\int_0^\pi d\theta P_k(\cos\theta)\sin\theta = 2\delta_{\rm k,0}, \tag{A4}$$

leads to:

$$\Psi(R) = \frac{\alpha^3}{\pi}\int_0^\infty dp\frac{\hat{g}_s(p)}{p}\int_0^\infty dre^{-\alpha r} r\sin pr\sin pR. \quad \text{(A5)}$$

Then, we use the inverse Fourier transform,

$$\hat{g}_s(p) = \int_0^\infty g(x)\sin px dx, \quad \text{(A6)}$$

to obtain, after some straightforward calculations, the following more useful form:

$$\begin{aligned}\Psi(R) =& \\ \frac{\alpha}{4}\Big\{&(1-\alpha R)e^{\alpha R}\left[\int_0^R dx\, g(x)\, e^{-\alpha x} - \int_0^\infty dx\, g(x)\, e^{-\alpha x}\right] \\ &-(1+\alpha R)e^{-\alpha R}\left[\int_0^R dx\, g(x)\, e^{\alpha x} - \int_0^\infty dx\, g(x)\, e^{-\alpha x}\right] \quad \text{(A7)} \\ &+\alpha e^{\alpha R}\left[\int_0^R dx\, g(x)\, x\, e^{-\alpha x} - \int_0^\infty dx\, g(x)\, x\, e^{-\alpha x}\right] \\ &+\alpha e^{-\alpha R}\left[\int_0^R dx\, g(x)\, x\, e^{\alpha x} + \int_0^\infty dx\, g(x)\, x\, e^{-\alpha x}\right]\Big\}\end{aligned}$$

In order to simplify this expression, we introduce an auxiliary function $\psi(x)$ that makes the integrals exact:

$$g(x) \equiv \psi(x) - \frac{2}{\alpha^2}\psi''(x) + \frac{1}{\alpha^4}\psi^{iv}(x) \quad \text{(A8)}$$

We can insert Eq (A8) into Eq. (A7) and, upon integration by parts, we get:

$$\Psi(R) = \psi(R) - (1+\frac{\alpha R}{2})e^{-\alpha R}\psi(0) + \frac{R}{2\alpha^2}e^{-\alpha R}\psi''(0) \quad \text{(A9)}$$

where ψ is a solution to the ordinary differential Eq. (A8) that satisfies the conditions of being an analytic function at $x = 0$, and

$$\lim_{x\to\infty} \psi^{(k)}(x)\, x\, \exp(-\alpha x) = 0\ ;\ k = 0,1,2,3 \quad \text{(A10)}$$

where $\psi^{(k)}(x)$ stands for $\psi(x)$ and its first three derivatives.

These conditions are easily fulfilled in all the cases of interest. Actually, the analyticity is satisfied in the Newtonian limit, that is the behaviour that we expect to recover at $R \sim 0$. Although it is possible to artificially build a *pathological* $\psi(x)$ such that it can represent a physical system without satisfying Eq. (A10), it can be seen that almost every function ψ that does not satisfy it corresponds to a rotation velocity that grows almost exponentially with the distance, which clearly seems to contradict the observations.

Actually, it is straightforward to see that, provided $\psi(R)$ is a solution to Eq. (A8), then $\Psi(R)$ is also a solution to the same equation. Moreover, the terms proportional to $\psi(0)$ and $\psi''(0)$ in Eq. (A9) assure that Ψ and its second derivative are both zero at the origin. Taking all this into consideration, we finally obtain that:

$$g(x) = \Psi(x) - \frac{2}{\alpha^2}\Psi''(x) + \frac{1}{\alpha^4}\Psi^{(iv)}(x), \quad \text{(A11)}$$

$$\Psi(0) = \Psi''(0) = 0. \quad \text{(A12)}$$

Once $\Psi(R)$ is known we can calculate $\Psi_{\rm eff}(R)$ using Eq. (9). Equivalently, once $g(r)$ is known, $g_{\rm eff}(r)$ can be obtained through Eq. (3). Using these two equations together with Eq. (A11), and after some straightforward calculations, we can find a direct relation between $g_{\rm eff}$ and $\Psi_{\rm eff}$:

$$\begin{aligned}g_{\rm eff}(x) =\ & \Psi_{\rm eff}(x) - \tfrac{2}{\alpha^2}\Psi''_{\rm eff}(x) + \tfrac{1}{\alpha^4}\Psi^{iv}_{\rm eff}(x) + \tfrac{4}{\alpha^2 x}\Psi'_{\rm eff}(x) \\ & - \tfrac{4}{\alpha^4 x^4}\left[2x\Psi'_{\rm eff}(x) - 2x^2\Psi''_{\rm eff}(x) + x^3\Psi'''_{\rm eff}(x)\right]\end{aligned} \quad \text{(A13)}$$

From the behaviour of Ψ at the origin (Eq. (A12), and Eq. (9)), it is easy to see that, at the origin, $\Psi_{\rm eff}$ will satisfy:

$$\Psi_{\rm eff}(0) = \Psi'_{\rm eff}(0) = \Psi''_{\rm eff}(0) = 0. \quad \text{(A14)}$$

(Eqs. (A11), (A12), (A13) and (A14) already appear in Sect. 3, but we prefer to rewrite them again here to keep the flow of the paper).

A.2. Thin-disk with exponential density

The line of reasoning for the solution of the problems outlined in Eqs. (18) and (19) is very similar to the one used in the case of the sphere. The use of the Fourier sine transform (Eq. (A1)) and the addition theorem for Bessel functions (Eq. (A2)) allows us to decouple the integration variables and arrive to an expression for Ψ that is slightly different from the one found in the spherical case:

$$\begin{aligned}\frac{\Psi(R)}{R} =\ & \frac{2\alpha^2}{\pi}\int_0^\infty dr\int_0^\infty dp\ \hat{g}_s(p)\ r\ e^{-\alpha r}\sum_{\rm k=0}^\infty (2k+1) \\ & \times \frac{J_{\rm k+\frac{1}{2}}(pR)}{\sqrt{R}}\frac{J_{\rm k+\frac{1}{2}}(pr)}{\sqrt{r}}\int_0^{2\pi} d\theta P_k(\cos\theta).\end{aligned} \quad \text{(A15)}$$

In this case, the absence of the $\sin\theta$ term in the volume element (that appears in the spherical case, but not for a thin disk) does not allow us to use the orthogonality of Legendre polynomials but the following expression:

$$\int_0^{2\pi} d\theta P_k(\cos\theta) = \begin{cases} 2\left[\frac{\Gamma(2k+1/2)}{\Gamma(2k+1)}\right]^2 & ;\ \text{if } k = 2n+1 \\ 0 & ;\ \text{if } k = 2n \end{cases}, \quad \text{(A16)}$$

and then Eq. (A15) becomes:

$$\begin{aligned}\Psi(R) =\ & -\frac{\alpha^2}{\pi\sqrt{R}}\sum_{\rm k=0}^\infty (4k+1)\left[\frac{\Gamma(2k+1/2)}{\Gamma(2k+1)}\right]^2 \\ & \times \int_0^\infty dp\frac{\hat{g}_s(p)}{p}J_{\rm 2k+1/2}(pR)\int_0^\infty dre^{-\alpha r}\sqrt{r}J_{\rm 2k+1/2}(pr)\end{aligned} \quad \text{(A17)}$$

We apply our approximation here. We only consider the first term in the series of Bessel functions, that is, we drop all the terms in the series but the one with $k = 0$. We have shown in Sect. 5 that in the Newtonian limit (i.e, when $g(r) = g_{\rm eff}(r) = 1$) this approximation corresponds to applying the Gauss' law to the mass distribution, i.e, to saying that the gravitational force at a distance R is proportional to the total mass contained in the sphere of radius R. This is the reason why we have called this method the "*Gaussian approximation*". As it is quite a good approximation in the Newtonian case, and we also have seen that it is exact for some forms of $g(r)$ and a very good approximation for the most interesting forms of $g(r)$, we restrict ourselves to consider only the first term in the series.

Thus, we write:

$$\Psi_0(R) = -\frac{\alpha^2}{\sqrt{R}} \int_0^\infty dp \frac{\hat{g}_s(p)}{p} J_{1/2}(pR) \times \int_0^\infty dr e^{-\alpha r} \sqrt{r} J_{1/2}(pr) \quad \text{(A18)}$$

Now, using the functional form of $J_{1/2}$,

$$J_{1/2}(x) = \sqrt{\frac{2}{\pi x}} \sin(x) \quad \text{(A19)}$$

and applying (A6) to invert the Fourier transformation, and after some straightforward calculations, we get:

$$\Psi_0(R) = -\frac{\alpha}{2} \left\{ e^{\alpha R} \left[\int_0^R dx g(x) e^{-\alpha x} - \int_0^\infty dx g(x) e^{-\alpha x} \right] - e^{-\alpha R} \left[\int_0^R dx g(x) e^{\alpha x} - \int_0^\infty dx g(x) e^{-\alpha x} \right] \right\}. \quad \text{(A20)}$$

At this point, it is useful to introduce an auxiliary function $\psi(x)$ that makes the integrals exact:

$$g(x) \equiv \psi(x) - \frac{1}{\alpha^2} \psi''(x). \quad \text{(A21)}$$

Eq (A21) can be inserted into Eq. (A20) and, upon integration by parts, we get:

$$\Psi_0(R) = \psi(R) - e^{-\alpha R} \psi(0), \quad \text{(A22)}$$

where ψ is a solution of the ordinary differential Eq. (A21) that satisfies the conditions of being an analytical function at $x = 0$, and

$$\lim_{x\to\infty} \psi(x) \exp(-\alpha x) = \lim_{x\to\infty} \psi'(x) \exp(-\alpha x) = 0. \quad \text{(A23)}$$

These conditions are easily satisfied in all the astrophysical systems. The analyticity is satisfied in the Newtonian limit, which is the behaviour we expect to recover at $R \sim 0$ and it can be seen that if Eq. (A23) were not satisfied, the rotation velocity would grow almost exponentially with the distance, which clearly seems to contradict the observations.

It is straightforward to see that, provided $\psi(R)$ is a solution of Eq. (A21), then $\Psi_0(R)$ is also a solution of the same equation. Moreover, the term proportional to $\psi(0)$ in Eq. (A22) implies that Ψ_0 is zero at the origin. Taking all that into account, we finally obtain:

$$g(x) = \Psi(x) - \frac{1}{\alpha^2} \Psi''(x), \quad \text{(A24)}$$

and

$$\Psi(0) = 0. \quad \text{(A25)}$$

where we have omitted the subscript 0 everywhere as we will in what follows.

Once $\Psi(R)$ is known, $\Psi_{\rm eff}(R)$ can be calculated using Eq. (9). Equivalently, once $g(r)$ is known, $g_{\rm eff}(r)$ can be obtained through Eq. (3). Using these two equations together with Eq. (A24), and after some straightforward calculations, a direct relation between $g_{\rm eff}$ and $\Psi_{\rm eff}$ can be obtained:

$$g_{\rm eff}(x) = \Psi_{\rm eff}(x) - \frac{1}{\alpha^2} \Psi''_{\rm eff}(x) + \frac{2}{\alpha^2 x} \Psi'_{\rm eff}(x). \quad \text{(A26)}$$

From Eq. (9) and the behaviour of Ψ at the origin, Eq. (A25), it is easy to see that, at the origin, $\Psi_{\rm eff}$ will satisfy:

$$\Psi_{\rm eff}(0) = \Psi'_{\rm eff}(0) = 0. \quad \text{(A27)}$$

References

Begeman K., 1987, Ph.D. Thesis, Groningen University.
Gradshteyn, I.S., Ryzhik, I.M., 1980, Table of Integrals, Series, and Products. Academic Press, p. 979
Kent S., 1987, AJ 93, 816
Kuhn J.R., Kruglyak L., 1987, ApJ 313,1
Mannheim P.D., Kazanas D., 1989, ApJ 342, 635
Rodrigo-Blanco C., Pérez-Mercader J., 1997, in press: "Rotation curves for spiral galaxies and non-Newtonian gravity: A phenomenological approach".
Tohline J.E., 1983, in Athanassoula E. (ed.), Internal kinematics and dynamics of galaxies, IAU Symp. 100, Reidel, Dordrecht, p. 205
Will C.M., 1993, Theory and experiment in gravitational Physics, Revised Edition. Cambridge University Press

This article was processed by the author using Springer-Verlag LaTeX A&A style file *L-AA* version 3.